

## Fluorescence and NMR Binding Studies of *N*-Aryl-*N*-(9-methylanthryl)diaza-18-crown-6 Derivatives

Anthony J. Pearson\* and Wenjing Xiao

Chemistry Department, Case Western Reserve University, Cleveland, Ohio 44106-7078

ajp4@po.cwru.edu

Received February 18, 2003

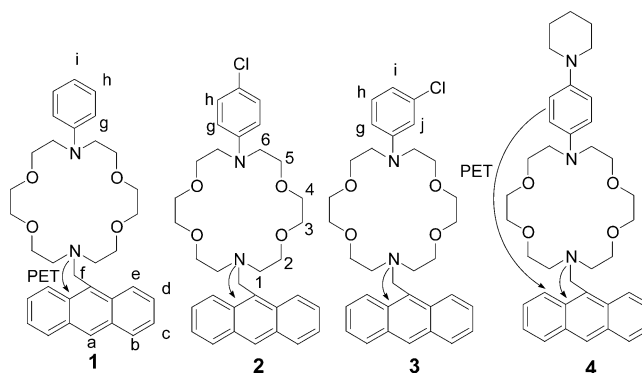
*N*-Aryl-*N*-(9-methylanthryl)diaza-18-crown-6 derivatives perform as fluorescent photoinduced electron-transfer (PET) sensors with very selective response toward  $\text{Ca}^{2+}$  versus  $\text{Mg}^{2+}$ ,  $\text{Na}^+$ , and  $\text{K}^+$ . The fluorescence intensity was increased by a factor of up to 170 in the presence of  $\text{Ca}(\text{ClO}_4)_2$ .  $^1\text{H}$  NMR studies show that metal cations affect these molecules very differently:  $\text{Ca}^{2+}$  has a global effect on each molecule, while  $\text{Mg}^{2+}$  affects part of each molecule, and  $\text{K}^+$  and  $\text{Na}^+$  affect each molecule moderately, which is very consistent with the fluorescence response.

### Introduction

Crown ethers are well-known for their excellent affinity toward alkali and alkaline earth metal cations.<sup>1</sup> Various fluorescent PET (photoinduced electron transfer) sensors containing crown ether moieties have been well-studied.<sup>2</sup> Diazacrown ether derivatives SBF1 and PBF1 are commercial  $\text{Na}^+$  and  $\text{K}^+$  fluorescent indicators.<sup>3</sup> We have made a number of *N*-aryl azacrown ether derivatives through our new synthetic methodology,<sup>4</sup> and preliminary studies indicated that this type of crown ether responded very selectively toward  $\text{Ca}^{2+}$  and  $\text{Mg}^{2+}$  versus  $\text{K}^+$  and  $\text{Na}^+$ .<sup>5</sup> Encouraged by this result, we have screened more *N*-aryl crown ether molecules and discovered that good-to-excellent selectivity toward  $\text{Ca}^{2+}$  over the other three cations can be achieved by simply introducing an *N*-phenyl group onto diaza-18-crown-6. So far most calcium-selective fluorescent sensors have a binding motif similar to that of BAPTA (1,2-bis-(2-aminophenoxy)ethane-*N,N,N,N*-tetraacetic acid).<sup>3,6</sup> In this paper we report the binding studies of novel calcium-selective fluorescent PET molecules from *N*-aryl crown ethers with a pendant anthracene through fluorescence and NMR spectroscopy.

**Fluorescence Studies.** Anthracene was chosen as the fluorescent probe because it has been widely used for fluorescent sensing studies.<sup>7</sup> The absorption and emission

### CHART 1



spectra of anthracene have been well-studied. Four PET molecules were synthesized conveniently by amination of 9-chloromethylanthracene with various *N*-aryl diaza-18-crown-6 derivatives.<sup>8</sup> Compounds **1–3** use the alkylamine as an electron donor, and compound **4** bears two electron donors: the alkylamine and the *p*-phenylenediamine moiety, which should each contribute to PET fluorescence quenching (Chart 1).

UV absorption and fluorescence emission spectra for **1–4** were obtained in the presence of  $\text{NaClO}_4$ ,  $\text{KClO}_4$ ,  $\text{Mg}(\text{ClO}_4)_2$ , and  $\text{Ca}(\text{ClO}_4)_2$  in  $\text{CH}_3\text{CN}$ . As expected, CHEF (chelation-enhanced fluorescence) was observed for all compounds upon addition of metal salts. All spectra were typical for anthracene compounds.<sup>7</sup> Figure 1 shows the absorption and emission spectra of **1** in the presence of  $\text{Ca}(\text{ClO}_4)_2$ . The absorption shows a major peak with  $\lambda_{\text{max}}$  at 254 nm and three minor peaks whose intensity is 20 times lower ( $\lambda_{\text{max}}$  at around 347, 366, and 386 nm). Metal perchlorates cause no shift but do elicit a slight decrease in the intensity of the major peak. The low-intensity

(1) (a) Inoue, Y.; Gokel, G. W. *Cation Binding by Macrocycles: Complexation of Cationic Species by Crown Ethers*; Marcel Dekker: New York, 1990. (b) Steed, J. W.; Atwood, J. L. *Supramolecular Chemistry*; Wiley: Chichester, UK, 2000.

(2) (a) Valeur, B.; Leray, I. *Coord. Chem. Rev.* **2000**, *205*, 3. (b) de Silva, A. P.; Fox, D. B.; Huxley, A. J. M.; Moody, T. S. *Coord. Chem. Rev.* **2000**, *205*, 41. (c) de Silva, A. P.; Gunaratne, H. Q. N.; Gunlaugsson, T.; Huxley, A. J. M.; McCoy, C. P.; Rademacher, J. T.; Rice, T. E. *Chem. Rev.* **1997**, *97*, 1515. (d) Desvergne, J. P.; Czarnik A. W. *Chemosensors of Ion and Molecule Recognition*; NATO ASI Series; Kluwer Academic Publishers: Dordrecht, The Netherlands, 1997.

(3) *Handbook of Fluorescent Probes and Research Products*, 9th ed.; web ed. at www.probes.com, 2002.

(4) Pearson, A. J.; Xiao W. *J. Org. Chem.* **2003**, *68*, 2161.

(5) (a) Pearson, A. J.; Hwang, J.-J.; Ignatov, M. E. *Tetrahedron Lett.* **2001**, *42*, 3537. (b) Pearson, A. J.; Hwang, J.-J. *Tetrahedron Lett.* **2001**, *42*, 3541.

(6) Czarnik A. W. *Fluorescent Chemosensors for Ion and Molecular Recognition*; American Chemical Society: Washington, DC, 1993; Chapter 9.

(7) (a) Huston, M. E.; Haider, K. W.; Czarnik, A. W. *J. Am. Chem. Soc.* **1988**, *110*, 4460. (b) Fages, F.; Desvergne, J.-P.; Kampke, K.; Bouas-Laurent, H.; Lehn, J.-P. M.; Meyer, M.; Albrecht-Gary, A.-M. *J. Am. Chem. Soc.* **1993**, *115*, 3658. (c) Fabbri, L.; Licchelli, M.; Pallavicini, P.; Taglietti, A. *Inorg. Chem.* **1996**, *35*, 1733. (d) Ojida, A.; Mito-oka, Y.; Inoue, M.; Hamachi, I. *J. Am. Chem. Soc.* **2002**, *124*, 6256.

(8) (a) Kubo, K.; Kato, N.; Sakurai, T. *Bull. Chem. Soc. Jpn.* **1997**, *70*, 3041. (b) de Silva, A. P.; de Silva, S. A. *J. Chem. Soc., Chem. Commun.* **1986**, 1709.

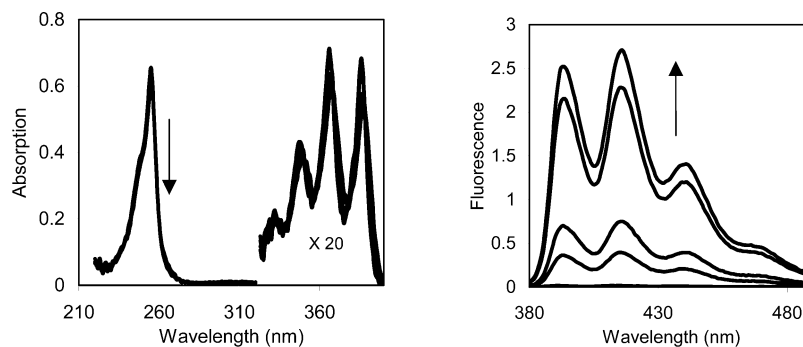


**FIGURE 1.** Absorption and emission spectra of **1** upon addition of  $\text{Ca}(\text{ClO}_4)_2$  ( $[\mathbf{1}] = 5.0 \mu\text{M}$ ,  $\lambda_{\text{Ex}} = 366 \text{ nm}$ ; equivalents of  $\text{Ca}(\text{ClO}_4)_2$  along the arrowed direction: 0, 0.5, 1, 5, 10).

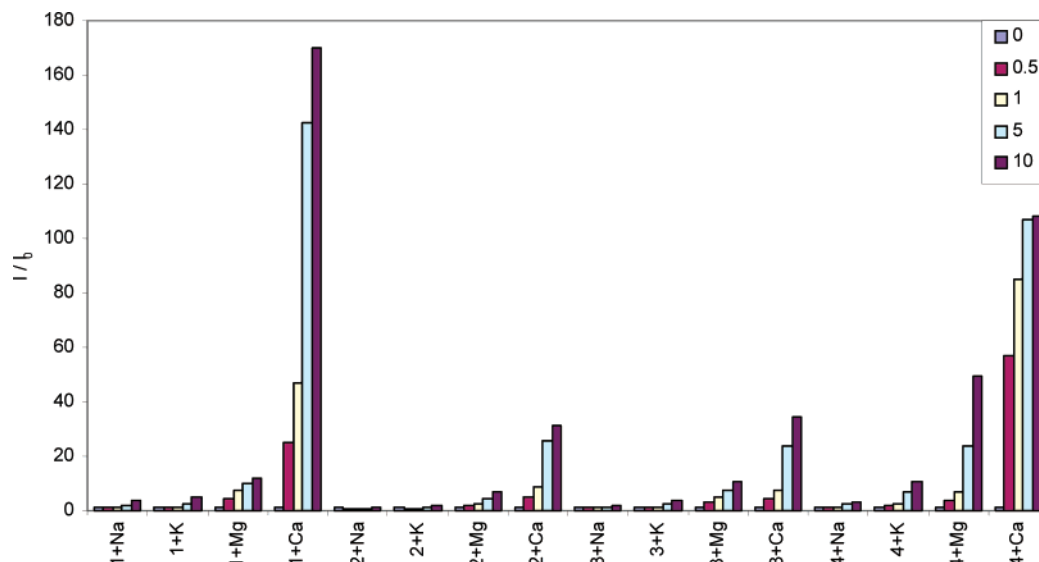


**FIGURE 2.** Change of fluorescence intensity upon addition of metal perchlorates ( $I/I_0$ : intensity in the presence/absence of metal salts; molar equivalent of metal salts: 0, 0.5, 1, 5, 10; concentration of **1–4**: 5, 10, 5, 10  $\mu\text{M}$ ; excited at 366 nm, emission maximum at 416 nm).

peaks undergo red shift (1 or 2 nm) and decrease of intensity upon addition of metal perchlorates. The fluorescence emission mirrors the minor peaks of the absorption, showing three peaks with  $\lambda_{\text{max}}$  at around 394, 416, and 440 nm, and the 416-nm peak has the highest intensity.

The changes in fluorescence emission intensities upon addition of metal perchlorates are collected in Figure 2. Up to 10 molar equiv, metal cations induce small red shifts (within 5 nm) of the emission maximum. All crown ether compounds respond more selectively toward  $\text{Ca}^{2+}$ ; **1** is the most selective one for which  $\text{Ca}^{2+}$  induces a huge increase in the emission intensity, while  $\text{Na}^+$ ,  $\text{K}^+$ , and  $\text{Mg}^{2+}$  have much smaller effects. The change for **4** is smaller than that for **1**, but is still dramatic, while **1** is better than **4** at discriminating between  $\text{Ca}^{2+}$  and  $\text{Mg}^{2+}$ . The intensity increase for **2** and **3** is similar, and is less than that for **4**, but they are more selective than **4** for  $\text{Ca}^{2+}$  over  $\text{Mg}^{2+}$ . The TAPD moiety in **4** is more electron rich than the phenyl groups in **1–3**, therefore more sensitive to  $\text{Mg}^{2+}$ , leading to poorer selectivity.

Relative fluorescence quantum yields were obtained by using quinine sulfate in 1.0 N  $\text{H}_2\text{SO}_4$  as the reference. The change of quantum yield is similar to that for emission intensity (Table 1). Compound **4** has the lowest quantum yield due to possible dual electron-transfer

**TABLE 1.** Fluorescence Quantum Yields ( $\Phi$  with/without 10 molar equiv of metal perchlorates) and Stability Constants ( $\log K$ , L/mol) in  $\text{CH}_3\text{CN}$

		<b>1</b>	<b>2</b>	<b>3</b>	<b>4</b>
$\text{Na}^+$	$\Phi_0$	0.001	0.004	0.004	0.0003
	F	0.007	0.006	0.008	0.0008
	$\log K$	4.4	3.2	6.1	3.6
$\text{K}^+$	F	0.006	0.009	0.014	0.0024
	$\log K$	6.6	2.6	3.8	4.3
$\text{Mg}^{2+}$	F	0.013	0.02	0.04	0.014
	$\log K$	6.7	3.5	4.7	5.9
$\text{Ca}^{2+}$	F	0.2	0.1	0.13	0.03
	$\log K$	5.2	4.7	5.0	6.8

pathways, even though the TAPD moiety is far away from the anthryl group. The stability constants are calculated from the absorption spectra based on the Lambert–Beer law (see ref 5a), but the values do not correlate very well with the corresponding fluorescence changes.

**NMR Studies.** NMR spectroscopy has been widely used for studying the binding between crown ethers and metal cations.<sup>9</sup> Coordination of the metal cation to the crown ether induces conformational reorganization of the ligand, and as a result, the chemical shifts and splitting patterns of the protons from the crown ether and the groups nearby undergo certain changes. Hence, monitor-

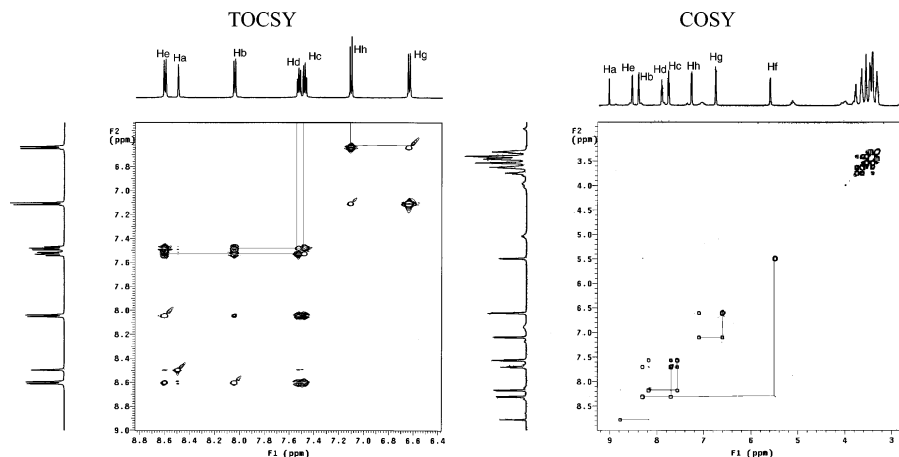


FIGURE 3. TOCSY spectra of **2** and COSY spectra of **2** in the presence of  $\text{Mg}(\text{ClO}_4)_2$  in  $\text{CD}_3\text{CN}$ .

TABLE 2.  $^1\text{H}$  NMR Chemical Shifts ( $\delta$ , ppm) and Coupling Constants ( $J$ , Hz) for Aromatic Moieties and the Bridging  $\text{CH}_2$  ( $\text{H}^j$ ) (see Chart 1 for proton label)

		$\text{H}^a$	$\text{H}^b$	$\text{H}^c$	$\text{H}^d$	$\text{H}^e$	$\text{H}^f$	$\text{H}^g$	$\text{H}^h$	$\text{H}^i$	$\text{H}^j$
<b>1</b>	$\delta$	8.50	8.04	7.53	7.47	8.61	4.60	6.68	7.16	6.62	
	$J$	s	d	dd	dd	d	s	d	dd	d	
<b>2</b>	$\delta$	8.50	8.05	7.53	7.48	8.60	4.59	6.64	7.11		
	$J$	s	d	dd	dd	d	s	d	d		
<b>3</b>	$\delta$	8.49	8.04	7.53	7.47	8.60	4.57	6.60	7.11	6.60	6.69
	$J$	s	d	dd	dd	d	s	dd	dd	dd	dd

ing the magnitude of the spectral change will provide further insight on how and where a metal cation binds to the ligand.

$^1\text{H}$  NMR spectra of **1–3** in  $\text{CD}_3\text{CN}$  were obtained in the absence and presence of various metal perchlorates. The chemical shifts and coupling constants for the anthracene and phenyl protons of the three compounds are listed in Table 2. Compounds **1–3** each have different substitutions on the phenyl ring, so it is easy to assign the phenyl protons based on splitting patterns and coupling constants. For example, in the case of **1**,  $\text{H}^g$  appears as a doublet, both  $\text{H}^h$  and  $\text{H}^i$  appear as doublets of doublets, and the integrations are 2:2:1 for  $\text{H}^g:\text{H}^h:\text{H}^i$ . For **2**, it is simpler, and both  $\text{H}^g$  and  $\text{H}^h$  appear as doublets.  $\text{H}^g$  is at higher field because of the ortho N substitution, while  $\text{H}^h$  is at lower field because of the ortho Cl substitution. For **3**, all four protons appear as doublets of doublets, but the coupling constants are very different:  $\text{H}^h$  has two relatively large couplings from  $\text{H}^g$  and  $\text{H}^i$ ;  $\text{H}^g$  and  $\text{H}^i$  each has a small coupling from  $\text{H}^j$ ; and  $\text{H}^j$  has two small couplings from  $\text{H}^g$  and  $\text{H}^i$ .

The anthracene moiety shows the same splitting patterns in all three compounds. The assignment of  $\text{H}^a$  to

$\text{H}^e$  is based on coupling constants and 2D spectra. TOCSY spectra of **2** clearly show the cross-peak between the  $\text{H}^b$  doublet and the  $\text{H}^c$  doublet of doublets, and between the  $\text{H}^d$  doublet of doublets and the  $\text{H}^e$  doublet (Figure 3). Addition of metal perchlorates does not change the coupling constants of the aromatic protons, therefore NOESY and COSY spectra of **2** in the presence of  $\text{Mg}(\text{ClO}_4)_2$  are also useful for assignment of the aromatic protons (Figure 3 displays part of the COSY spectrum). Both COSY and NOESY spectra of **2**/ $\text{Mg}(\text{ClO}_4)_2$  show clearly the cross-peaks between the  $\text{H}^a$  singlet and the  $\text{H}^b$  doublet,  $\text{H}^b$  doublet and the  $\text{H}^c$  doublet of doublets,  $\text{H}^d$  doublet of doublets and the  $\text{H}^e$  doublet, and the  $\text{H}^e$  doublet and the  $\text{H}^f$  doublet.

It was found that spectra of **2** are the same in the presence of 1 molar equiv or 5 molar equiv of metal salts, indicating that **2** forms 1:1 complexes with metal perchlorates at a given concentration. It is assumed that **1** and **3** also form 1:1 complexes under similar conditions. Each metal salt affects the spectra in the same way for **1** to **3**: each metal causes similar changes on the chemical shifts of the same groups for all three compounds, with some notable exceptions. Figure 4A–C summarizes in graph form the changes in the chemical shifts of the aromatic protons and the spacer  $\text{CH}_2$  protons. In the presence of metal perchlorates, most resonances undergo a downfield shift due to the deshielding effect of the bound metal cation, which reduces the electron density of the heteroatom in the crown ether and of the aromatic  $\pi$  system. The anthracene proton  $\text{H}^e$  moves upfield, and this unique feature is likely due to possible C–H $\cdots$ O (from the crown ether 13-position) hydrogen bonding,

(9) (a) Bordunov, A. V.; Bradshaw, J. S.; Zhang, X. X.; Dalley, N. K.; Kou X.; Izatt, R. M. *Inorg. Chem.* **1996**, *35*, 7229. (b) Bartsch, R. A.; Hwang, H.-S.; Talanov, V. S.; Talanov, G. G.; Purkiss, D. W. *J. Org. Chem.* **1999**, *64*, 5341. (c) Fedorova, O. A.; Fedorov, Y. V.; Verdernikov, A. I.; Gromov, S. P.; Yescheulova, O. V.; Alifimov, M. V. *J. Phys. Chem. A* **2002**, *106*, 6213. (d) Trippé, G.; Levillain, E.; Le Derf, L.; Gorgues, A.; Sallé, M.; Jeppesen, J. O.; Nielsen, K.; Becher, J. *Org. Lett.* **2002**, *4*, 2461. (e) Esteban D.; Avecilla, F.; Platas-Iglesias, C.; Mahía, J.; de Blas, A.; Rodríguez-Blas, T. *Inorg. Chem.* **2002**, *41*, 4337. (f) Costero, A. M.; Andreu, R.; Monrabal, E.; Martínez-Mañez, R.; Sancenón, F.; Soto, J. *J. Chem. Soc., Dalton Trans.* **2002**, 1769.

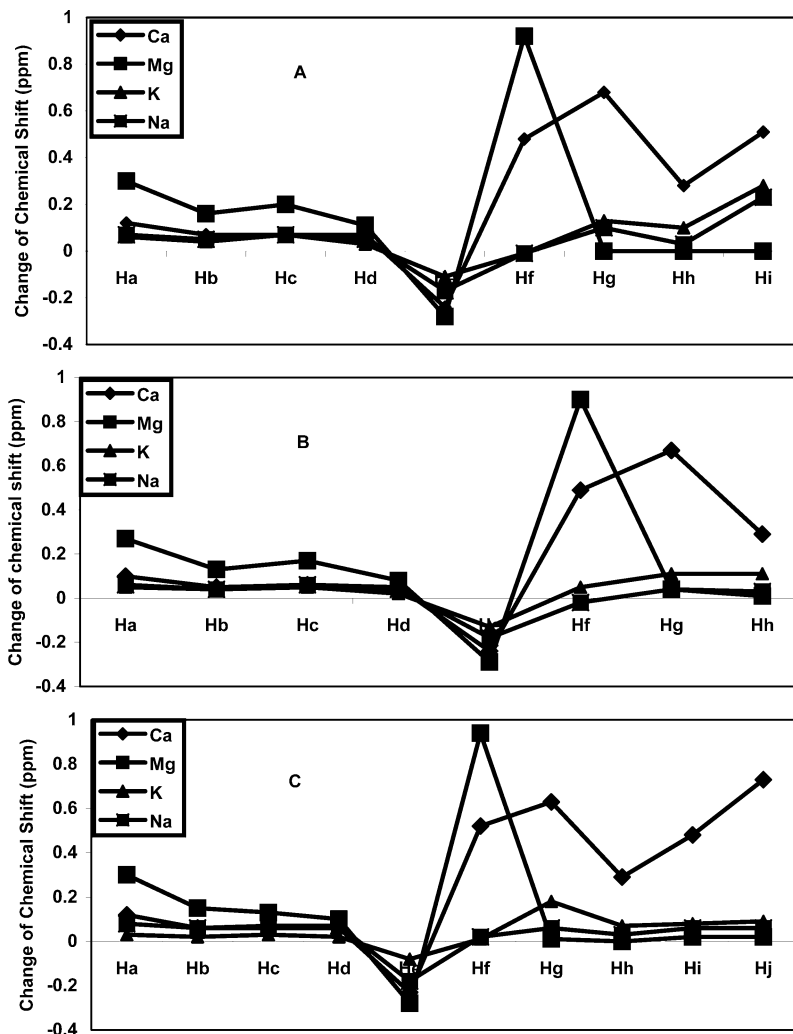


**FIGURE 4.**  $^1\text{H}$  NMR chemical shift changes ( $\Delta\delta$  ppm) for selected protons from **1** (A), **2** (B), and **3** (C) in the presence of metal perchlorates (see Chart 1 for proton labels).

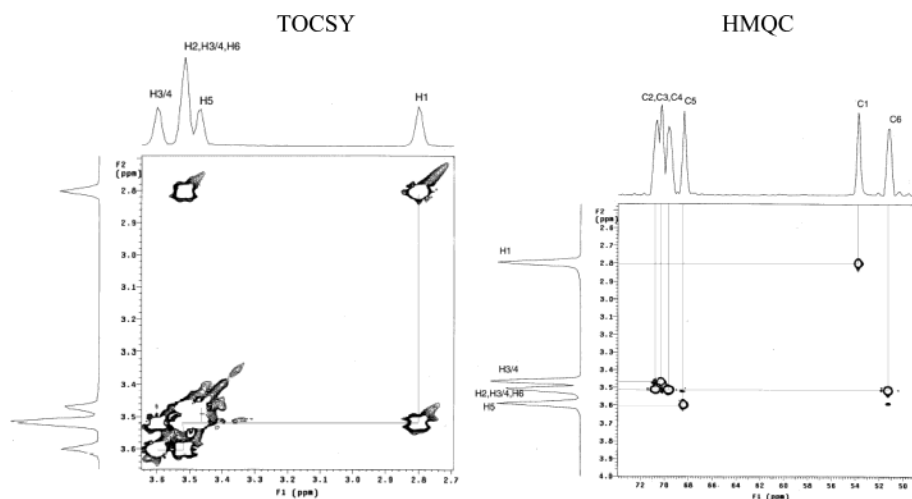


**FIGURE 5.** TOCSY and HMQC spectra of **2** (crown ether part) in  $\text{CD}_3\text{CN}$ .

which is broken upon metal binding, leading to a less deshielding effect from the oxygen atom.<sup>10</sup>  $\text{Mg}^{2+}$  induces the largest change on the anthracene protons (up to 0.3 ppm) and the methylene  $\text{CH}_2 - \text{H}^f$  (up to 0.9 ppm), but its effect on the phenyl protons is the least.  $\text{Ca}^{2+}$  causes the largest increase on the phenyl proton chemical shifts

(up to 0.7 ppm), and increases the  $\text{H}^f$  chemical shifts (0.5 ppm) less than does  $\text{Mg}^{2+}$  but much greater than do  $\text{K}^+$  and  $\text{Na}^+$ .  $\text{Ca}^{2+}$ ,  $\text{K}^+$ , and  $\text{Na}^+$  induce similar changes on

(10) Meadows, E. S.; De Wall, S. L.; Barbour, L. J.; Fronczek, F. R.; Kim, M.-S.; Gokel, G. W. *J. Am. Chem. Soc.* **2000**, *122*, 3325.

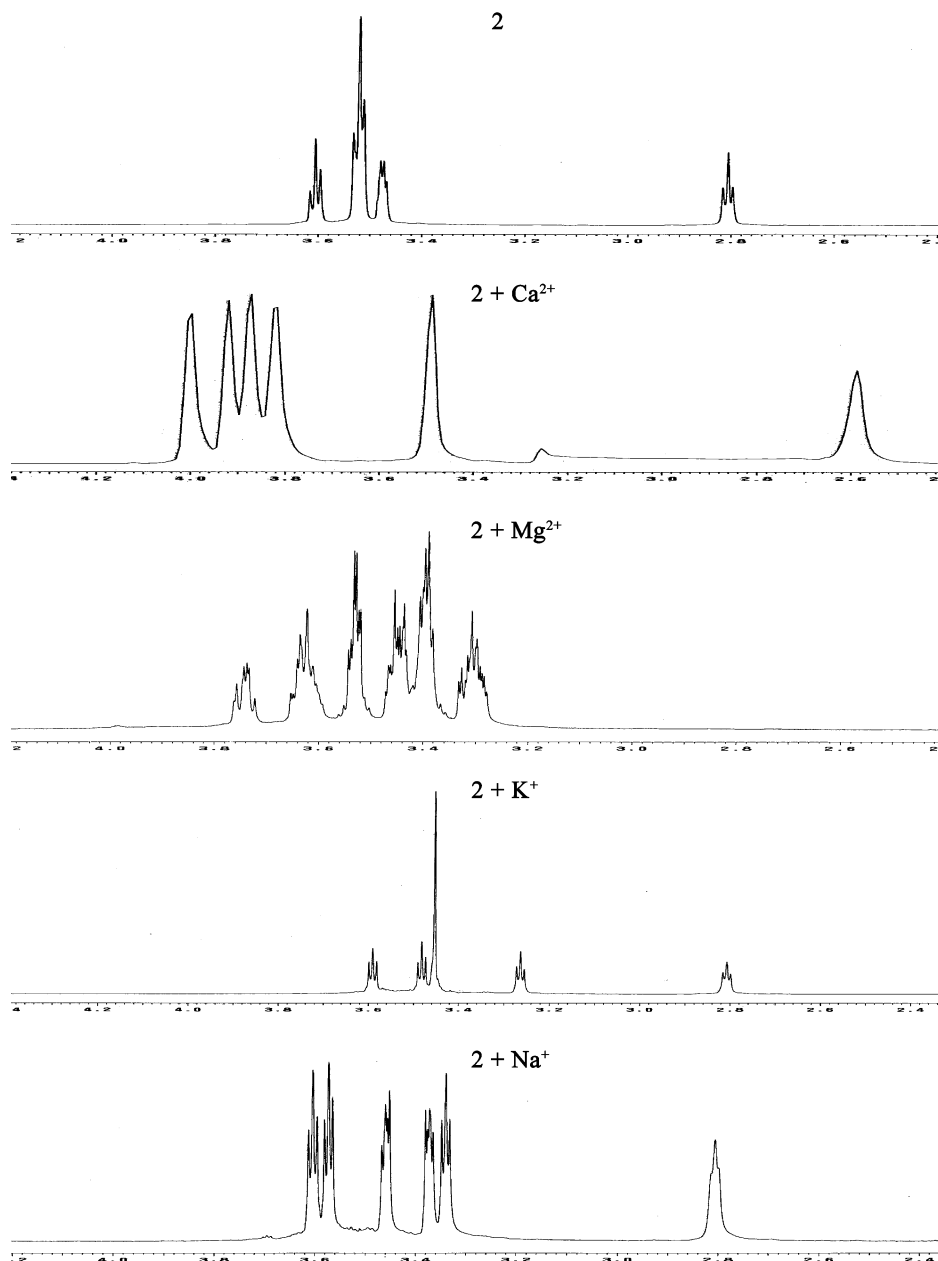


**FIGURE 6.**  $^1\text{H}$  NMR spectra of **2** (crown ether part) in the absence and presence of metal perchlorates in  $\text{CD}_3\text{CN}$ .

the anthracene protons, but these are less than for  $\text{Mg}^{2+}$ .  $\text{K}^+$  causes a slightly larger increase than does  $\text{Na}^+$  on the phenyl proton chemical shifts. The magnitude of change for each phenyl proton is very different in the presence of  $\text{Ca}^{2+}$ . In compounds **1** and **2**,  $\text{Ca}^{2+}$  induces the largest change on  $\text{H}^g$ , and in compound **3**,  $\text{Ca}^{2+}$  induces the largest change on  $\text{H}^g$  and  $\text{H}^j$ , probably due to the fact that  $\text{H}^g$  (and  $\text{H}^j$ ) is close to the crown ether cavity.

The crown ether protons also show similar patterns in all three compounds. In symmetrically substituted diaza-18-crown-6, the 24 protons usually fall into three groups ( $8\text{H} \times 3$ ).<sup>19</sup> In our *N*-aryl diazacrown ethers, the two crown ether nitrogen atoms are different: an alkylamine and an arylamine. As a result, the 24 protons should be differentiated into six groups, though the middle peaks could overlap with each other, and the actual spectra show four peaks. For example, the 24

protons of **2** are divided into four groups: 3.61 (4H, t,  $J = 6.0$  Hz), 3.52 (12H), 3.48 (4H), 2.80 ppm (4H, t,  $J = 5.7$  Hz) (Figure 6). The TOCSY spectrum shows three cross-peaks between the 3.52-ppm group and each of the other three peaks (Figure 5). The 2.8-ppm triplet can be assigned to  $\text{H}^1$  easily according to available data on the  $\alpha$ -alkyl protons of a tertiary amine.<sup>11</sup> Therefore  $\text{H}^2$  should be in the 3.52-ppm group. In the HMQC spectra, the 54.0-ppm peak can be assigned to  $\text{C}^1$  since it is correlated to the 2.8-ppm triplet. The 51.6-ppm peak was then assigned to  $\text{C}^6$  because the carbon neighboring an amine nitrogen should appear at higher field than the carbon neighboring an ether oxygen. The  $\text{C}^6$  peak (51.6 ppm) correlates with the 5.2-ppm group, indicating  $\text{H}^6$  is in the multiplet, therefore the 3.61-ppm triplet belongs to  $\text{H}^5$ ,

(11) Crews, P.; Rodriguez, J.; Jaspars, M. *Organic structure analysis*, Oxford University Press: New York, 1998; Chapter 4.

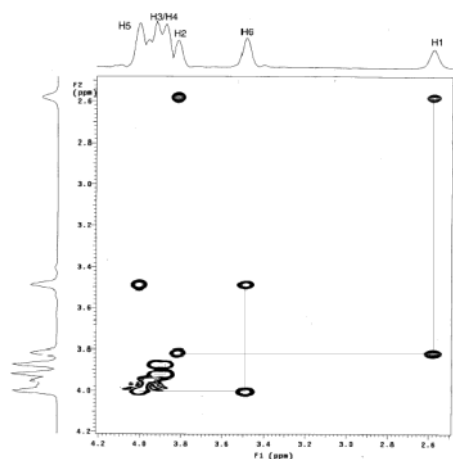


**FIGURE 7.** TOCSY spectra of **2** (crown ether part) in the presence of  $\text{Ca}(\text{ClO}_4)_2$  in  $\text{CD}_3\text{CN}$ .

and the correlated 68.4-ppm peak can be assigned to  $\text{C}^5$ . The 70-ppm peak was tentatively assigned to  $\text{C}^2$ . The 70.4- and 70.6-ppm peaks can be assigned to either  $\text{C}^3$  or  $\text{C}^4$ , and the 3.48-ppm group can be assigned to either  $\text{H}^3$  or  $\text{H}^4$ , as can part of the 3.52-ppm group (Figure 5).

The changes in chemical shifts and splitting patterns for the crown ether protons depend greatly on the metal salts and are more complicated than the aromatic protons (Figure 6). While no attempt was made to assign all the peaks, it is clear that cation binding leads to differentiation (asymmetry) of the crown ether protons, indicating a significant conformational reorganization of the crown ether upon metal binding.

In the presence of  $\text{Ca}^{2+}$ , the crown ether protons of **2** show six groups of peaks, the center undergoes about 0.4 ppm downfield shift, and each peak is broad with no defined multiplicity, indicating a dynamic binding process. All six peaks can be assigned based on the assignments for **2** and the cross-peaks appearing in the TOCSY spectrum (Figure 7):  $\delta$   $\text{H}^1$  (2.58 ppm);  $\text{H}^2$  (3.82 ppm);  $\text{H}^{3\text{or}4}$  (3.89 or 3.93 ppm);  $\text{H}^6$  (3.49 ppm);  $\text{H}^5$  (4.00 ppm).

A remarkable observation is that the  $\text{H}^f$  singlet of **2** and **3** becomes a doublet ( $J = 6.6$  Hz) in the presence of  $\text{Mg}^{2+}$ , while the  $\text{H}^f$  singlet of **1** becomes a doublet ( $J = 1.8$  Hz) in the presence of  $\text{Ca}^{2+}$ . In the case of **2** with  $\text{Mg}(\text{ClO}_4)_2$ , the doublet appears with identical peak separation (Hz) in both 200- and 600-MHz spectra. The HOMO2DJ spectrum unambiguously shows that the doublet is due to  $J$  coupling (Figure 8), not two species. The coupling constant from HOMO2DJ is identical with the value calculated from the two 1D spectra. We were unable to assign this coupling based on COSY spectral data, but the NOESY spectrum shows two cross-peaks between the  $\text{CH}_2$  and two crown ether protons (Figure 8)—a stronger cross-peak to the multiplet at around 3.63 ppm and a weaker cross-peak to the multiplet at around 3.40 ppm—and the two peaks are assigned to the  $\text{H}^1$  protons from the crown ether ring based on extensive 2D NMR experiments, indicating that this unusual coupling is likely a long-range coupling between the methylene  $\text{CH}_2$  and one of the  $\text{H}^1$  protons. The  $\text{H}^f$  doublet for **1** in the presence of  $\text{Ca}^{2+}$  and the doublet for **3** in the presence of  $\text{Mg}^{2+}$  are assumed to have the same origin as for **2**/ $\text{Mg}(\text{ClO}_4)_2$ .

In the presence of  $\text{Mg}^{2+}$ , the crown ether protons of **2** also show six groups of peaks (from low to high field: 2H, 4H, 4H, 4H, 6H, 4H), each of which is shown as a multiplet with a very complicated splitting pattern. The  $^{13}\text{C}$  NMR spectra of **2** with and without  $\text{Mg}(\text{ClO}_4)_2$  show different chemical shifts for most peaks. As a control, the  $^1\text{H}$  NMR spectra of 9-chloromethylantracene with and without  $\text{Mg}(\text{ClO}_4)_2$  were also recorded, and the two spectra are identical, indicating that  $\text{Mg}^{2+}$  has no effect on the anthracene system in the absence of the crown ether.

Extensive 2D NMR studies made it possible to assign almost every proton of **2** complexed with  $\text{Mg}(\text{ClO}_4)_2$  (Figure 9). HMQC indicates that some of the geminal  $\text{CH}_2$  protons in the crown ether are differentiated. The four  $\text{H}^1$  on  $\text{C}^1$  (54.2 ppm), the four  $\text{H}^2$  on  $\text{C}^2$  (63.4 ppm), the four  $\text{H}^3$  on  $\text{C}^3$  (70.0 ppm), and the four  $\text{H}^4$  on  $\text{C}^4$  (70.8 ppm) each appear as two groups, while  $\text{H}^5$  on  $\text{C}^5$  (68.6 ppm) and  $\text{H}^6$  on  $\text{C}^6$  (51.2 ppm) each remain in one peak. The collective data indicate that  $\text{Mg}^{2+}$  binds closer to the anthracene side of the crown ether. Binding of  $\text{Mg}^{2+}$  to the crown ether is strong, but slow dynamics (on/off) compared to the NMR time scale produces two faces on the crown ether ring that are not averaged. The protons on the bound face and the nonbound face of the crown ether are in different chemical environments, and therefore they show different chemical shifts and splitting patterns. There are two cross-peaks for  $\text{H}^f$  protons and the crown ether  $\text{H}^1$  protons in the NOESY spectrum, indicating different types of  $\text{H}^1$  protons. There are two cross-peaks for the phenyl  $\text{H}^g$  and the crown ether protons in the NOESY spectrum, which are assigned to  $\text{H}^5$  and  $\text{H}^6$ . It is possible that the  $\text{C}^6\text{H}^6$  grouping is forced to adopt a position such that the crown ether nitrogen is conjugated with the phenyl ring, and doing so brings  $\text{H}^g$  into close contact with both  $\text{H}^5$  and  $\text{H}^6$ . The cross-peaks for the crown ether protons in COSY and NOESY are consistent with this assignment. Combined with the HOMO2DJ spectrum, the peaks can be assigned as follows:  $\delta$  (ppm)  $\text{H}^2$  (3.75),  $\text{H}^{2'}$  (3.63),  $\text{H}^1$  (3.63),  $\text{H}^{1'}$  (3.40),  $\text{H}^{3/4}$  (3.45),  $\text{H}^{3'/4'}$  (3.32),  $\text{H}^5$  (3.54),  $\text{H}^6$  (3.40).

In the presence of  $\text{K}^+$ , the crown ether protons of **2** show five groups of peaks. The tentative assignment is as follows:  $\delta$  (ppm) 3.59 ( $\text{H}^5$ , t,  $J = 4.8$  Hz), 3.48 ( $\text{H}^2$ , t,  $J = 4.8$  Hz), 3.45 ( $\text{H}^3$  and  $\text{H}^4$ ), 3.26 ( $\text{H}^6$ , t,  $J = 4.8$  Hz), 2.81 ( $\text{H}^1$ , t,  $J = 4.8$  Hz). In the presence of  $\text{Na}^+$ , the crown ether protons of **2** also show six groups of peaks, with the following tentative assignment:  $\delta$  (ppm) 3.60 ( $\text{H}^5$ , t,  $J = 4.8$  Hz), 3.58 ( $\text{H}^2$ , t,  $J = 4.8$  Hz), 3.46 ( $\text{H}^4$ , t,  $J = 4.5$  Hz), 3.38 ( $\text{H}^3$ , t,  $J = 4.5$  Hz), 3.34 ( $\text{H}^6$ , t,  $J = 4.8$  Hz), 2.81 ( $\text{H}^1$ , br).

Compound **1** shows spectral patterns similar to those for **2** in the presence of the same metal perchlorates; **3** also shows spectral patterns similar to those for **2** in the presence of  $\text{Ca}(\text{ClO}_4)_2$  and  $\text{Mg}(\text{ClO}_4)_2$ , and slightly different patterns in the presence of  $\text{KClO}_4$  and  $\text{NaClO}_4$ . In the presence of  $\text{KClO}_4$ , the  $\text{H}^5$  and  $\text{H}^2$  triplets of **3** partially overlap, but are distinguishable ( $J = 5.4$  Hz),  $\text{H}^3$  and  $\text{H}^4$  appear as AB systems, while  $\text{H}^1$  and  $\text{H}^6$  each still remain as a triplet ( $J = 5.4$  Hz). With  $\text{NaClO}_4$ , the  $\text{H}^5$  and  $\text{H}^2$  triplets overlap,  $\text{H}^3$  and  $\text{H}^4$  each appear as a multiplet,  $\text{H}^6$  overlaps with one multiplet of  $\text{H}^3$  and  $\text{H}^4$ , and  $\text{H}^1$  remains as a triplet ( $J = 5.4$  Hz).

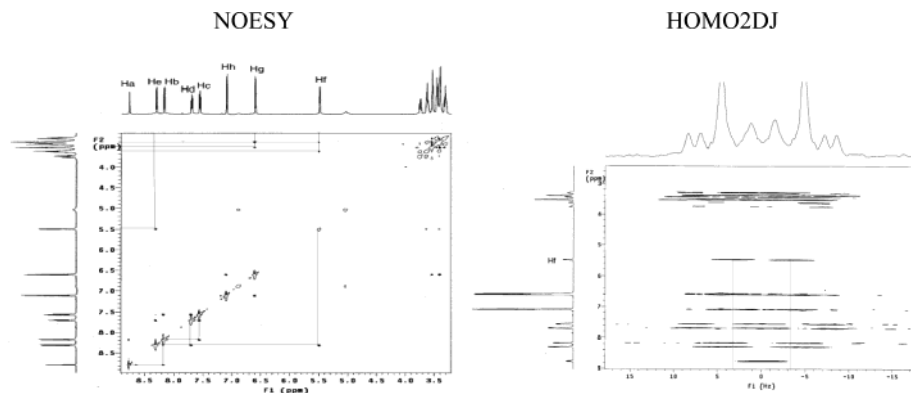


**FIGURE 8.** NOESY and HOMO2DJ spectra of **2** in the presence of  $\text{Mg}(\text{ClO}_4)_2$  in  $\text{CD}_3\text{CN}$ .

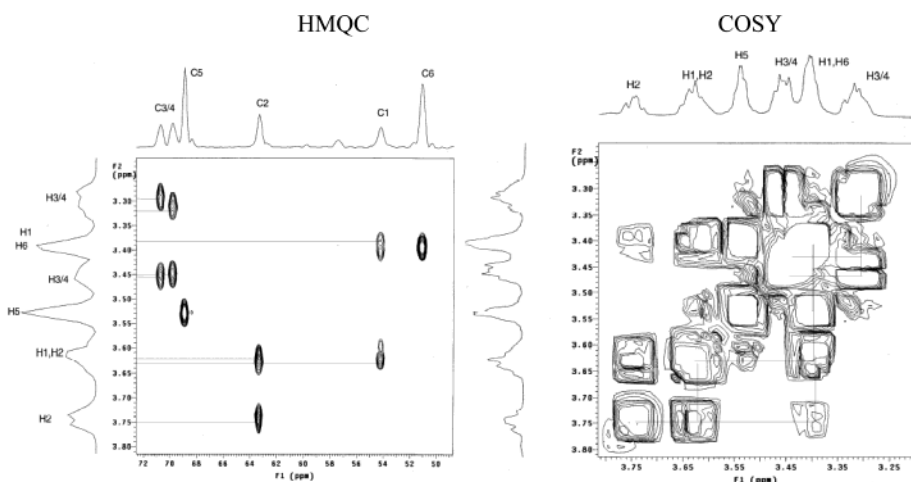


**FIGURE 9.** HMQC and COSY spectra of **2** (crown ether) in the presence of  $\text{Mg}(\text{ClO}_4)_2$  in  $\text{CD}_3\text{CN}$ .

## Discussion

Size-match often plays a very important role in the binding of crown ethers and metal cations.<sup>1</sup> In general,  $\text{Na}^+$  and  $\text{Ca}^{2+}$  fit well in both 15-crown-5 and 18-crown-6, and  $\text{K}^+$  fits best in 18-crown-6, while  $\text{Mg}^{2+}$  is too small for either one. A number of azacrown ethers with pendant aromatic groups have been studied, and in most cases size match between the crown ether cavity and metal cation is the key factor for selective binding.<sup>12</sup> In cases where size match is not the key factor, a number of other features have to be considered, such as substitution and topology of the crown ether, and the charge density of metal cations, etc. Compared with known azacrown ethers having an aromatic substituent, the very different fluorescence response from our new 9-anthrylmethyl armed azacrown ethers indicates that direct arylation on the amine nitrogen of diaza-18-crown-6 leads to significantly different binding properties. Apparently size-match cannot completely explain the fluorescence behavior of **1–4**.

It has been observed that the *N*-aryl  $\pi$  system is more sensitive toward higher charge density of metal cations.<sup>5,13</sup> Conjugation of the nitrogen lone pair with the

phenyl ring reduces the availability of the lone pair, and the requirement of coplanarity of the nitrogen substituents and the phenyl ring could limit the flexibility of the crown ether. The electron density of the phenyl ring also influences the selectivity. The best selectivity was observed with **1**, in which a simple phenyl ring is attached to the crown nitrogen atom. A more electron-rich (such as in **4**) or less electron-rich (such as in **2** and **3**) phenyl ring reduces the selectivity. Apparently the substitution on the phenyl ring of the crown ether plays a very important role in binding selectivity.

Among the four metal cations,  $\text{Mg}^{2+}$  has the highest charge density, but it is too small to fit snugly into any of the 18-crown-6 derivatives. The chemical shift change induced by  $\text{Mg}^{2+}$  indicates that it binds closer to the anthracene side of the crown ether, with little or no close contact to the phenyl side. The complicated spectral pattern of the crown ether moiety and the unusual  $\text{H}^f$  doublet from **2** and **3** in the presence of  $\text{Mg}^{2+}$  suggests that  $\text{Mg}^{2+}$  binding causes a significant conformational reorganization of the crown ether. The large but unsymmetrical effect of  $\text{Mg}^{2+}$  on the NMR spectrum and the small effect of  $\text{Mg}^{2+}$  on the fluorescence indicates that  $\text{Mg}^{2+}$  is probably dislodged from the binding site upon formation of the excited state, because the binding is not strong enough to compete with the PET process, which reduces the availability of the nitrogen lone pair.<sup>14</sup>

(12) (a) de Silva, A. P.; de Silva, S. A. *J. Chem. Soc., Chem. Commun.* **1986**, 1709. (b) Jang, H.; Nakamura, K.; Yi, S.; Kim, J.; Go, J.; Yoon, J. *J. Inclusion Phenom. Macrocyclic Chem.* **2001**, *40*, 313. (c) Kubo, K.; Sakurai, T. *Chem. Lett.* **1996**, 959. (d) Kubo, K.; Ishige, R.; Sakurai, T. *Heterocycles* **1998**, *48*, 347. (e) Bourson, J.; Pouget, J.; Valeur, B. *J. Phys. Chem.* **1993**, *97*, 4552.

(13) Street, K. W., Jr.; Krause, S. A. *Anal. Lett.* **1986**, *19*, 735.

Another possibility is that the small  $Mg^{2+}$  cation moves closer to the phenyl side of the crown ether after photoexcitation, so it cannot inhibit the PET efficiently (this would correspond to a vibrational movement of the Mg–crown complex, which would occur more rapidly than a translational exit of the Mg from the crown). This is possible only because  $Mg^{2+}$  is small compared with the crown ether cavity.

$K^+$  fits better in the above 18-crown-6 ligands, which is shown from the moderate change on the chemical shifts of both sides of the crown ether, but  $K^+$  has the lowest charge density. This compromise leads to a rather weak binding, which is unable to modulate the PET process. Compared with  $K^+$ ,  $Na^+$  has higher charge density but less effective size match, therefore it cannot prevent the PET process either.

Compared with  $K^+$ ,  $Na^+$ , and  $Mg^{2+}$ ,  $Ca^{2+}$  is the most suitable for both size-match and charge-density sensitivity of the *N*-aryl moiety.  $Ca^{2+}$  induces large changes on the chemical shift of both halves of the crown ether, and especially the aniline group. The relatively large downfield shift of the crown ether protons upon  $Ca^{2+}$  addition indicates a strong interaction between the positive charge on  $Ca^{2+}$  and the crown ether ring. Unlike  $Mg^{2+}$ ,  $Ca^{2+}$  binds strongly to the alkylamine nitrogen even in the excited state, leading to inhibition of the PET process. The global effect of  $Ca^{2+}$  on the ligand certainly contributes to the selective fluorescence response.

## Conclusions

NMR studies provide binding information in the ground state, and fluorescence response relates the events after photoexcitation. Here a very consistent match was observed from the two methods. For these *N*-aryl diaza-18-crown-6 derivatives, the structure of the crown ether, the charge density of metal cation, and size match between the crown ether cavity and metal cation are all important factors for strong binding and selective fluorescence response.

## Experimental Section

**General Procedure for Anthracene Attachment.** The amine<sup>4</sup> and 9-chloromethylanthracene were dissolved in  $CH_3CN$ , and  $Et_3N$  (excess) was added. The mixture was refluxed overnight. The solution was filtered through Celite, and the solvent was removed by rotary evaporation. The residue was purified by silica gel flash chromatography.<sup>7,8</sup>

**7-Anthracen-9-ylmethyl-16-phenyl-1,4,10,13-tetraoxa-7,16-diazacyclooctadecane (1).** Flash chromatography ( $CH_2Cl_2$ /hexanes/ $Et_3N$  1/5/0.1,  $R_f$  0.4) afforded the product as an orange waxy solid in 70% yield. <sup>1</sup>H NMR (600 MHz,  $CD_3CN$ )  $\delta$  8.61 (2H, d,  $J = 9.0$ ), 8.50 (1H, s), 8.04 (2H, d,  $J = 8.4$ ), 7.53 (dd,  $J = 9.0, 6.0$ ), 7.47 (dd,  $J = 8.4, 6.0$ ), 7.16 (2H, dd,  $J = 8.4, 7.2$ ), 6.68 (1H, t,  $J = 7.2$ ), 6.62 (2H, d,  $J = 8.4$ ), 4.60 (2H, s), 3.62 (4H, t,  $J = 6.0$ ), 3.53 (12H), 3.48 (4H), 2.82 (4H, t,  $J = 6.0$ ). <sup>13</sup>C NMR (75 MHz,  $CD_3COCD_3$ )  $\delta$  149, 132.4, 132.3, 131.7, 130, 129.9, 129.8, 129.7, 129.6, 128.1, 126.5, 126.3, 125.8, 125.6, 116.4, 116.3, 112.4, 71.7, 71.2, 70.7, 69.5, 54.6, 51.9. HRMS-FAB calcd for  $C_{33}H_{40}O_4N_2$  528.2988, found  $MH^+$  529.3081.

**7-Anthracen-9-ylmethyl-16-(4-chlorophenyl)-1,4,10,13-tetraoxa-7,16-diazacyclooctadecane (2).** Flash chromatography ( $CH_2Cl_2$ /hexanes/ $Et_2O$  4/16/1;  $R_f$  0.3) afforded the product as a yellow-green waxy solid in 78% yield. <sup>1</sup>H NMR (600,

$CD_3CN$ )  $\delta$  8.60 (2H, d,  $J = 9.0$ ), 8.50 (1H, s), 8.05 (2H, d,  $J = 8.4$ ), 7.53 (2H, dd,  $J = 9.0, 6.6$ ), 7.48 (2H, dd,  $J = 8.4, 6.6$ ), 7.11 (2H, d,  $J = 9.0$ ), 6.64 (2H, d,  $J = 9.0$ ), 4.60 (2H, s), 3.61 (4H, t,  $J = 6.0$ ), 3.52 (12H), 3.48 (4H, t,  $J = 3.6$ ), 2.81 (4H, t,  $J = 5.7$ ). <sup>13</sup>C NMR (50 MHz,  $CDCl_3$ )  $\delta$  146.6, 131.5, 130.5, 129.0, 127.5, 125.6, 125.3, 124.9, 120.7, 112.9, 71.1, 70.6, 70.3, 68.8, 53.9, 51.5. HRMS-FAB calcd for  $C_{33}H_{39}O_4N_2Cl$  562.2598, found 562.2598.

**7-Anthracen-9-ylmethyl-16-(3-chlorophenyl)-1,4,10,13-tetraoxa-7,16-diazacyclooctadecane (3).** Flash chromatography ( $CH_2Cl_2$ /hexanes/ $Et_3N$  6/12/1,  $R_f$  0.6) afforded the product as an orange waxy solid in 78% yield. <sup>1</sup>H NMR (600 MHz,  $CD_3CN$ )  $\delta$  8.60 (2H, d,  $J = 9.0$ ), 8.49 (1H, s), 8.04 (2H, d,  $J = 8.4$ ), 7.52 (2H, dd,  $J = 9.0, 6.6$ ), 7.48 (2H, dd,  $J = 8.4, 6.6$ ), 7.11 (1H, dd,  $J = 7.8, 7.8$ ), 6.69 (1H, dd,  $J = 2.1, 1.8$ ), 6.60 (2H, dd,  $J = 7.8, 2.1$ ), 4.57 (2H, s), 3.61 (4H, t,  $J = 5.7$ ), 3.52 (12H), 3.47 (4H), 2.80 (4H, t,  $J = 6.0$ ). <sup>13</sup>C NMR (50 MHz,  $CD_3COCD_3$ )  $\delta$  150.5, 135.7, 132.6, 132.4, 131.8, 129.8, 128.3, 126.6, 126.5, 125.9, 116.0, 112.1, 111.1, 71.9, 71.3, 70.8, 69.5, 54.7, 52.4, 52.2. HRMS-FAB calcd for  $C_{33}H_{39}O_4N_2Cl$  562.2598, found  $MH^+$  563.2662.

**7-Anthracen-9-ylmethyl-16-(4-piperidin-1-yl-phenyl)-1,4,10,13-tetraoxa-7,16-diazacyclooctadecane (4).** Flash chromatography (hexanes/ $CH_2Cl_2$ / $Et_3N$  25/12/1,  $R_f = 0.5$ ) afforded the product as a yellow-green solid in 69% yield: mp 105–107 °C; <sup>1</sup>H NMR (300 MHz,  $CDCl_3$ )  $\delta$  8.59 (1H, d,  $J = 1.3$ ), 8.58 (1H, d,  $J = 1.3$ ), 8.41 (1H, s), 8.01 (1H, d,  $J = 1.3$ ), 7.98 (1H, d,  $J = 1.3$ ), 7.4–7.6 (4H), 6.88 (2H, d,  $J = 9.2$ ), 6.65 (2H, d,  $J = 9.2$ ), 4.61 (2H, s), 3.4–3.7 (20H), 2.8–3.0 (8H), 1.5–1.8 (6H); <sup>13</sup>C NMR (50 MHz,  $CDCl_3$ )  $\delta$  143.9, 142.7, 131.5, 131.4, 130.5, 129.0, 127.5, 125.6, 125.3, 124.9, 119.3, 113.2, 71.0, 70.6, 70.3, 69.3, 53.9, 52.7, 51.9, 51.8, 26.3, 24.3. HRMS-FAB calcd for  $C_{38}H_{49}O_4N_3$  611.3723, found 611.3753.

**Binding Studies.** NMR binding studies were carried out in  $CD_3CN$ . All NMR spectra were recorded on a 600-MHz instrument. Chemical shifts are reported in ppm with solvent as the internal reference, and coupling constants are reported in Hz. The average concentration for 1–3 is 10 mg/0.5 mL of  $CD_3CN$  (~0.05 M). Five molar equivalents of metal salts were added to ensure an excess amount of metal cation in the solution, leading to saturated complexation of the crown ethers so that the maximum effect could be observed. The actual amount for  $KClO_4$  is lower than the added amount due to limited solubility of  $KClO_4$  in  $CD_3CN$ . It was observed that addition of 1 drop of  $D_2O$  to the  $KClO_4$  solution does not change the spectrum, therefore introduction of unknown amounts of water in  $CD_3CN$  (much less than a drop, absorbed by the solvent during handling) was allowed to obtain a clear solution. <sup>1</sup>H NMR spectra for 4 with metal perchlorates are not informative because the spectra undergo broadening upon addition of metal salts, and the color of the solution turns blue. It is speculated that trace amounts of perchloric acid are formed from the metal perchlorate, which promotes the formation of the Würster's Blue radical cation from TAPD (tetraalkylphenylenediamine). Addition of base, such as  $Et_3N$ , turns off the blue color, indicating that the radical cation disappears upon quenching the acid.

Fluorescence binding studies were carried out as described in ref 5a.

**Acknowledgment.** The donors of the American Chemical Society Petroleum Research Fund are gratefully acknowledged for financial support. We thank Prof. Barkley for access to UV–visible and fluorescence instruments and Mr. Michael Ignatov for valuable help with the spectral studies.

**Supporting Information Available:** Titration spectra of UV absorption and fluorescence emission (2–4) and <sup>1</sup>H NMR spectra with (1–3) and without (1–4) different metal perchlorates. This material is available free of charge via the Internet at <http://pubs.acs.org>.

(14) Létard, J. F.; Lapouyade, R.; Rettig, W. *Pure Appl. Chem.* **1993**, *65*, 1705.